Figures and figure supplements

The signaling lipid sphingosine 1-phosphate regulates mechanical pain

Rose Z Hill *et al*

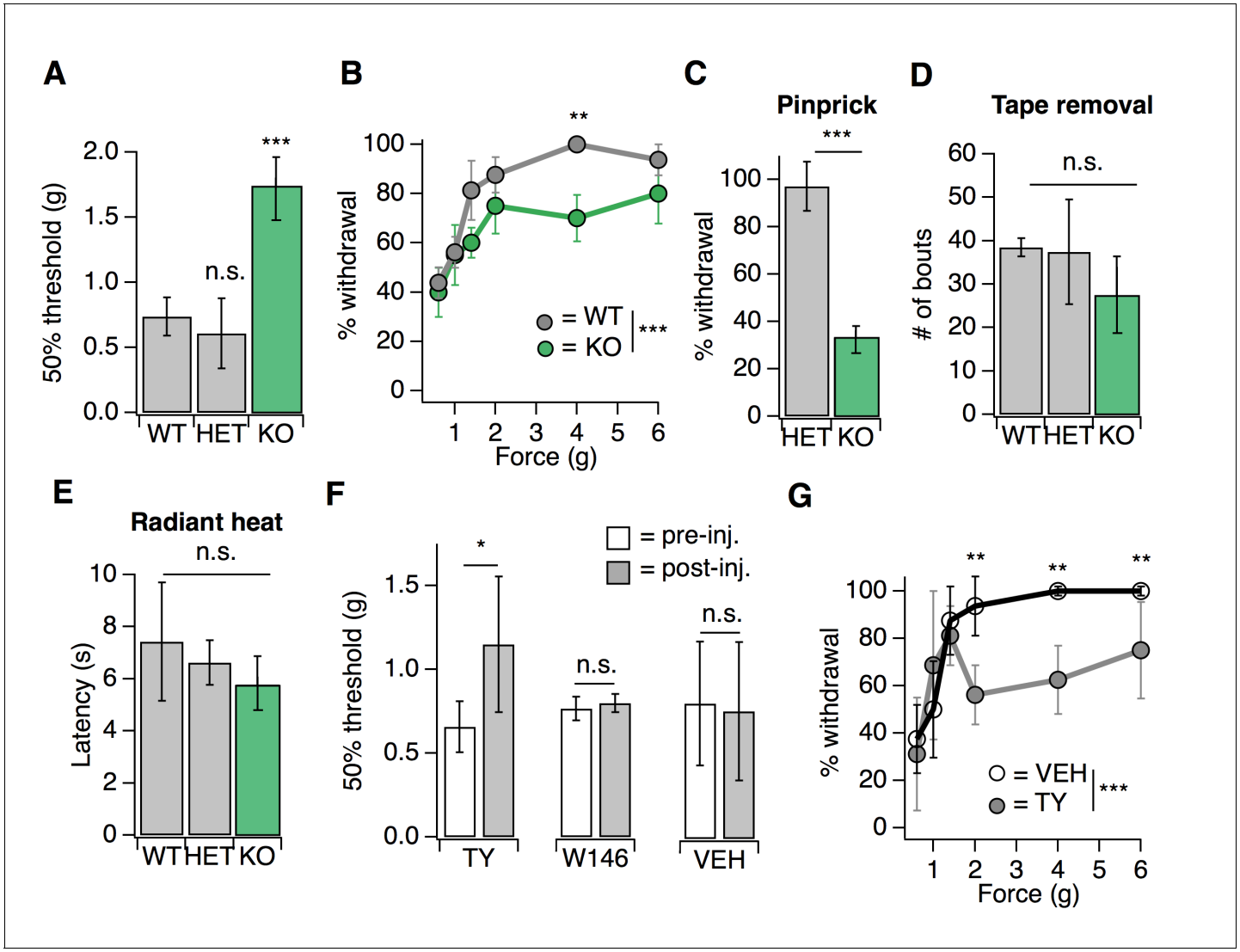

Figure 1. S1PR3 mediates acute mechanical pain. (**A**) von Frey 50% withdrawal threshold measurements for *S1pr3*$^{+/+}$ (WT, N = 8), *S1pr3*$^{+/-}$ (HET, N = 7) and *S1pr3*$^{-/-}$ (KO, N = 12) mice. p<0.0001 (one-way ANOVA). Tukey-Kramer post hoc comparisons for KO and HET to WT indicated on graph. (**B**) von Frey force-response graph for WT (N = 8) versus KO (N = 12) animals; $p_{genotype}$ <0.0001 (two-way ANOVA). Tukey HSD comparisons between genotypes are indicated for given forces. (**C**) % withdrawal to pinprick stimulation of hindpaw for HET versus KO animals; p<0.0001 (unpaired t-test; N = 5–7 mice per group). (**D**) Number of attempted removal bouts in tape assay for WT (N = 2), HET (N = 2), and KO (N = 5) mice; p=0.172 (one-way ANOVA). (**E**) Baseline radiant heat measurements for WT (N = 8), HET (N = 3), and KO (N = 5) mice; *p*=0.444 (one-way ANOVA). (**F**) von Frey 50% withdrawal threshold measurements for mice pre- and post-injection of 500 µM TY 52156 (N = 10), 10 µM W146 (N = 6), or 1% DMSO-PBS vehicle (N = 17); p=0.016, 0.650 (two-tailed paired t-test comparing vehicle- vs. drug-injected paw). (**G**) von Frey force-response graph for mice injected with either 1% DMSO-PBS (N = 4) or 500 µM TY 52156 (N = 4); $p_{treatment}$ <0.0001 (two-way ANOVA). Tukey HSD comparisons were made between treatment groups and significant differences at a given force are indicated on graph. Error bars represent mean ± SD.

DOI: https://doi.org/10.7554/eLife.33285.002

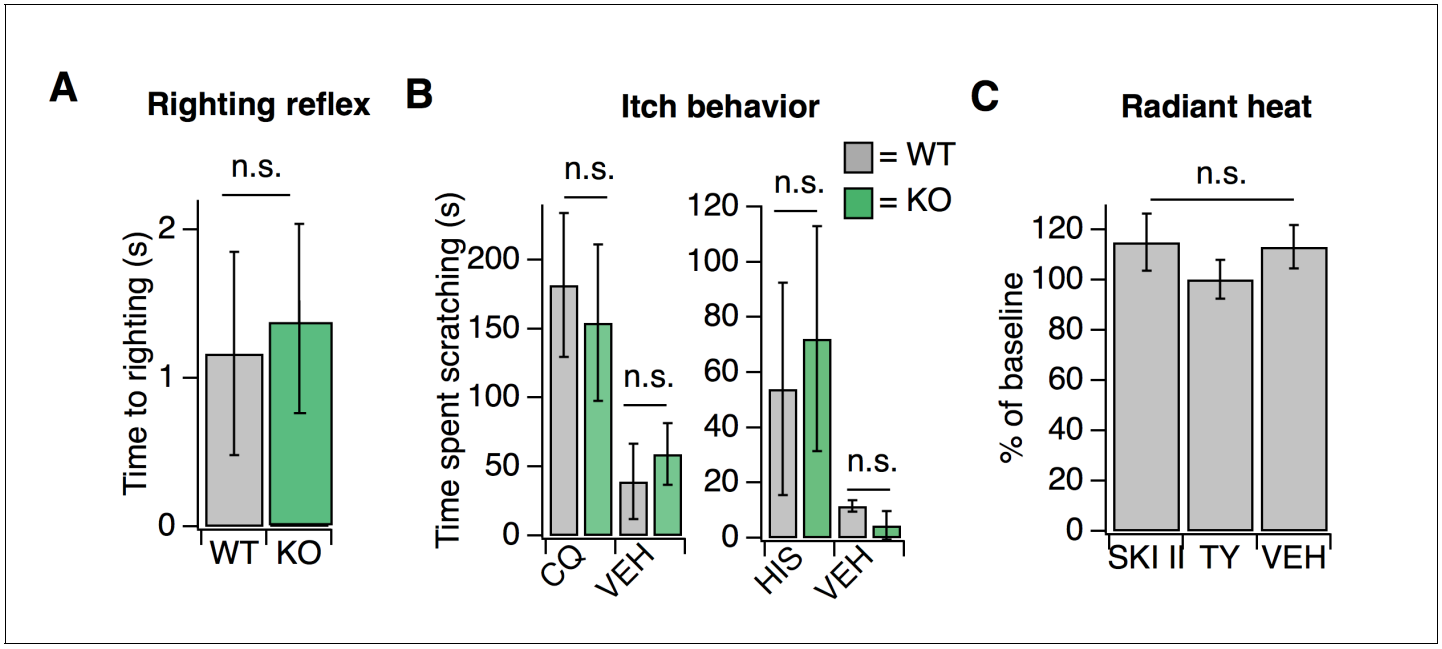

Figure 1—figure supplement 1. Loss of S1PR3 selectively impairs mechanonociception. Related to ***Figure 1***. (**A**) Time to righting in seconds for P7 pups per genotype for WT and KO mice; p=0.575 (two-tailed unpaired t-test; N = 7 mice per genotype). (**B**) (Left) Time spent scratching in response to injection of 50 mM chloroquine or PBS vehicle (VEH) in WT and KO mice; p=0.36, 0.98, (unpaired t-tests; N = 3–4 mice per group). (Right) Time spent scratching in response to injection of 27 mM Histamine or 0.1% DMSO-PBS in WT and KO mice; p=0.51, 0.06 (unpaired t-tests; N = 3–4 mice per group). (**C**) Normalized paw withdrawal latencies post-injection of SKI II, TY 52156, or 0.1% DMSO-PBS vehicle into the hind paw of wild-type animals; p=0.65 (one-way ANOVA; N = 5 mice per group). Unless otherwise indicated, error bars represent mean ± SD.

DOI: https://doi.org/10.7554/eLife.33285.003

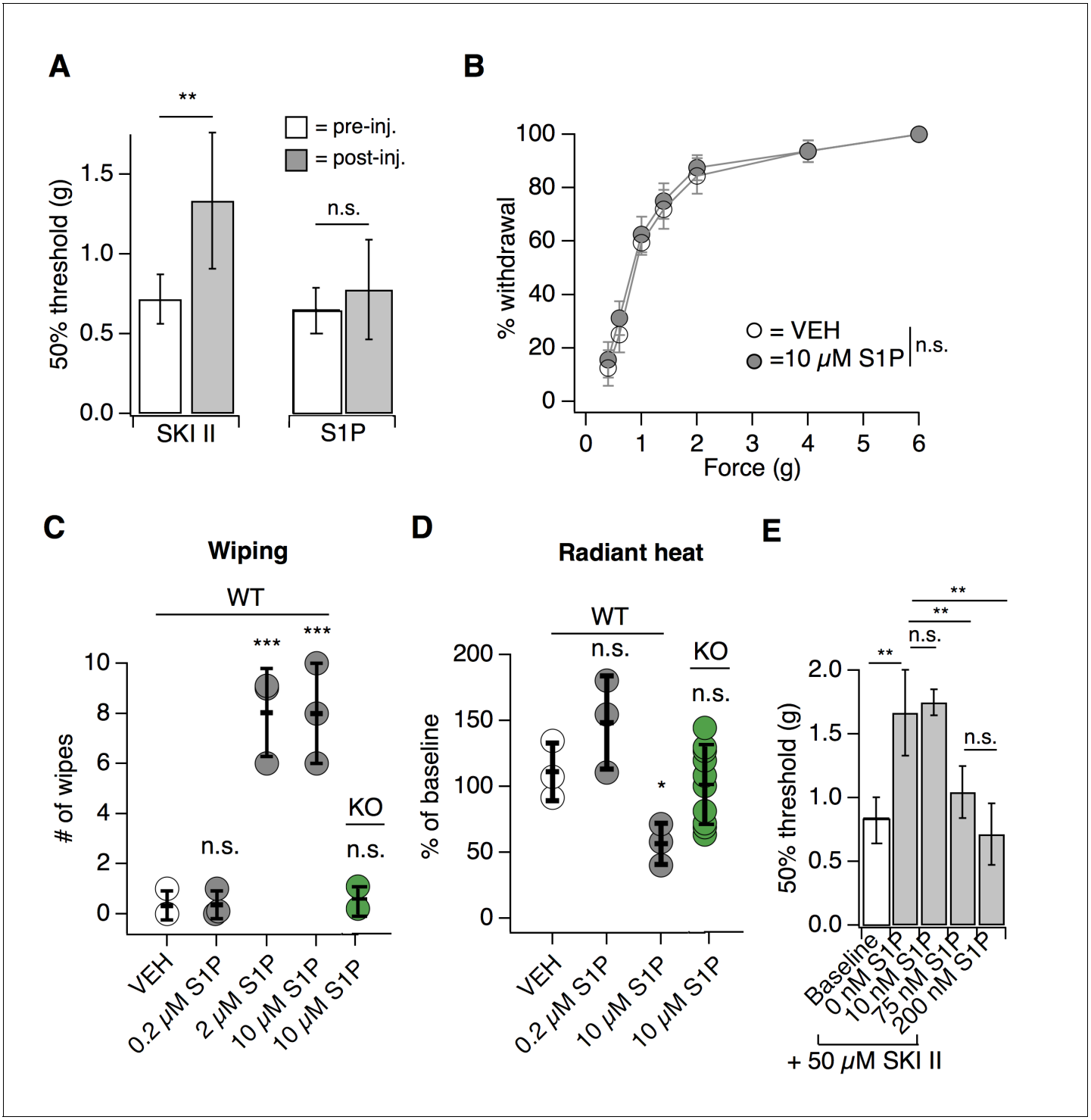

Figure 2. Endogenous S1P mediates acute mechanical pain. (**A**) von Frey 50% withdrawal measurements for mice pre- and post-injection of 50 µM SKI II (N = 8) or 10 µM S1P (N = 7); p=0.003, 0.604 (two-tailed paired t-tests). (**B**) von Frey force-response graph for animals injected with 10 µM S1P or 0.1% MeOH-PBS; $p_{genotype}$ >0.05 (two-way ANOVA; N = 8 mice per group). No Tukey HSD comparisons at any force between genotypes were significant. (**C**) Intradermal cheek injection of 10 µM S1P, 2 µM, 0.2 µM, and 20 µL 0.3% methanol PBS (vehicle), with quantification of number of forepaw wipes over the 5 min post-injection interval; $p<0.0001$ (one-way ANOVA; N = 3 mice per condition). Dunnett's multiple comparisons *p*-values are represented on graph for comparisons made between treated and vehicle groups. (**D**) Radiant heat normalized paw withdrawal latencies 20–30 min post injection of 15 µL 10 µM S1P, 0.2 µM S1P. or 0.3% methanol-PBS vehicle (i.d.) into the hind paw of S1PR3 WT or KO mice; p=0.0129 (one-way ANOVA; N = 3–10 mice per condition). Dunnett's multiple comparisons *p*-values are represented on graph for comparisons made between treated and vehicle groups. (**E**) von

Figure 2 continued on next page

Figure 2 continued

Frey 50% withdrawal measurements for mice pre- (baseline) and post-injection of 50 μM SKI II (N = 14) and 0 (N = 4), 10 (N = 3), 75 (N = 4), or 200 nM S1P (N = 3; one-way ANOVA; p=0.0001). Tukey Kramer comparisons are indicated on graph. Error bars represent mean ± SD.

DOI: https://doi.org/10.7554/eLife.33285.005

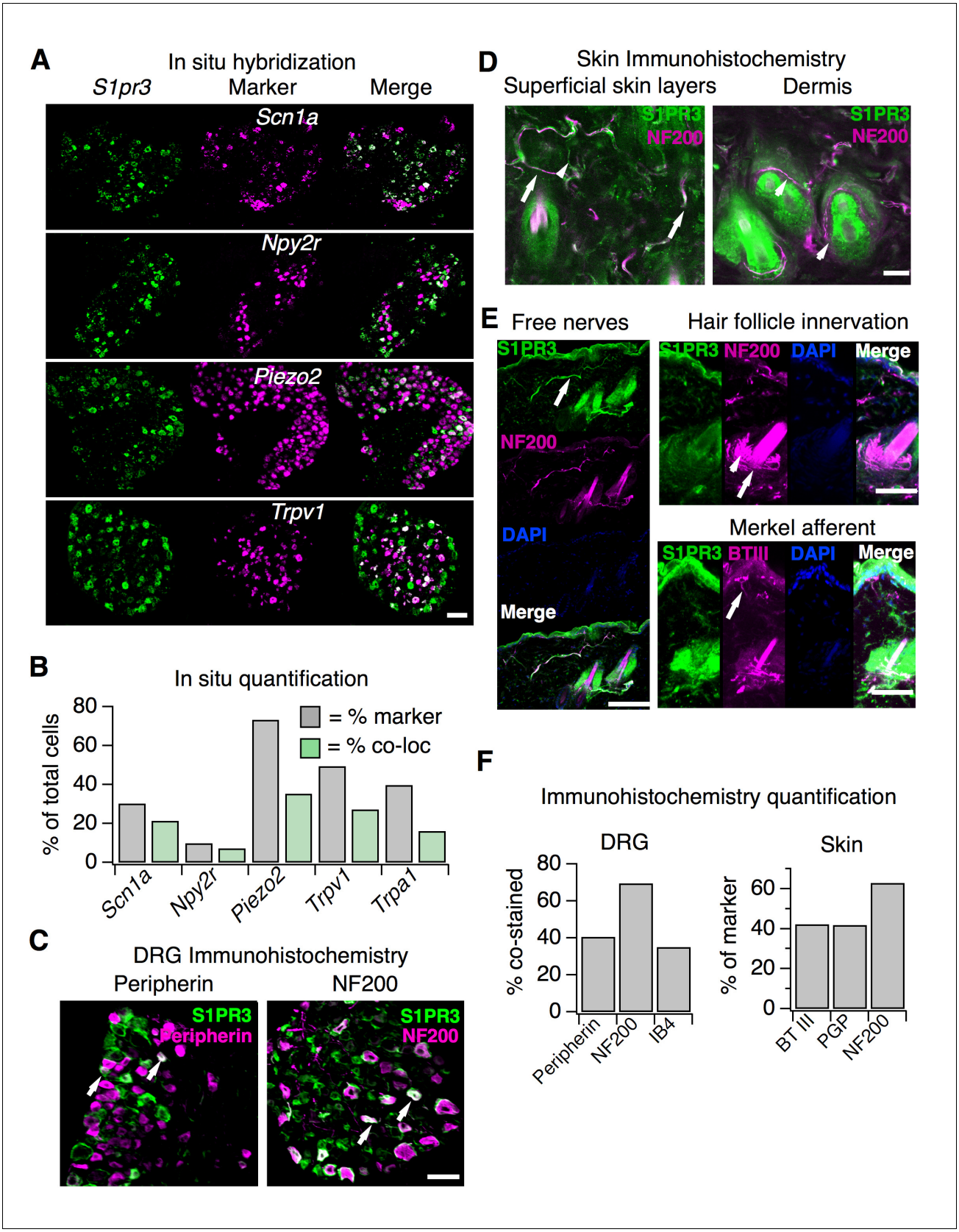

Figure 3. *S1pr3* is expressed in A mechanonociceptors and C thermal nociceptors. (**A**) (Top) Representative co-ISH of *S1pr3* (green; left) with *Scn1a*, *Npy2r*, *Piezo2*, and *Trpv1* (magenta; center) in sectioned DRG. Right column: overlay with co-localized regions colored white (10x air objective;

Figure 3 continued on next page

Figure 3 continued

scale = 100 μm). (**B**) Bar chart showing the % of total cells expressing the indicated marker (grey) and the % of total cells co-expressing both marker and *S1pr3* (green). See Table S1 for quantification. (**C**) Representative IHC images of sectioned DRG from *S1pr3*$^{mCherry/+}$ animals stained with anti-DsRed (green, S1PR3) and anti-Peripherin (left, magenta) or anti-NF200 (right, magenta). Arrows indicate co-stained cells. Images were acquired using a 10x air objective (scale = 100 μm). (**D**) Whole-mount skin IHC confocal images with anti-DsRed antibody (S1PR3, green) and anti-NefH antibody (NF200, magenta) in an *S1pr3*$^{mCherry/+}$ animal (20x water objective; scale = 50 μm). Arrows indicate co-positive free nerves (left image). Arrowheads indicate NF200- free nerves (left) or S1PR3- circumferential fibers (right image). (**E**) Sectioned skin IHC with anti-DsRed (S1PR3) and anti-NefH (NF200, left, top right) or anti-DsRed (S1PR3) and anti-beta-tubulin III (BTIII, bottom right) antibody (magenta) in *S1pr3*$^{mCherry/+}$ skin (20x air objective; scale = 50 μm). Arrows indicate co-positive free nerve endings (left), S1PR3-negative lanceolate/circumferential hair follicle endings (top right, arrow = circumferential, arrowhead = lanceolate), or S1PR3-negative putative Merkel afferent (bottom right). (**F**) (Left) Quantification of sectioned DRG IHC experiments showing % of S1PR3+ cells that co-stained with indicated markers (n > 250 cells per marker). (Right) Quantification of sectioned skin IHC experiments showing % of fibers positive for indicated marker that co-stained with S1PR3 (anti-DsRed; n = 10 images per marker from two animals).

DOI: https://doi.org/10.7554/eLife.33285.007

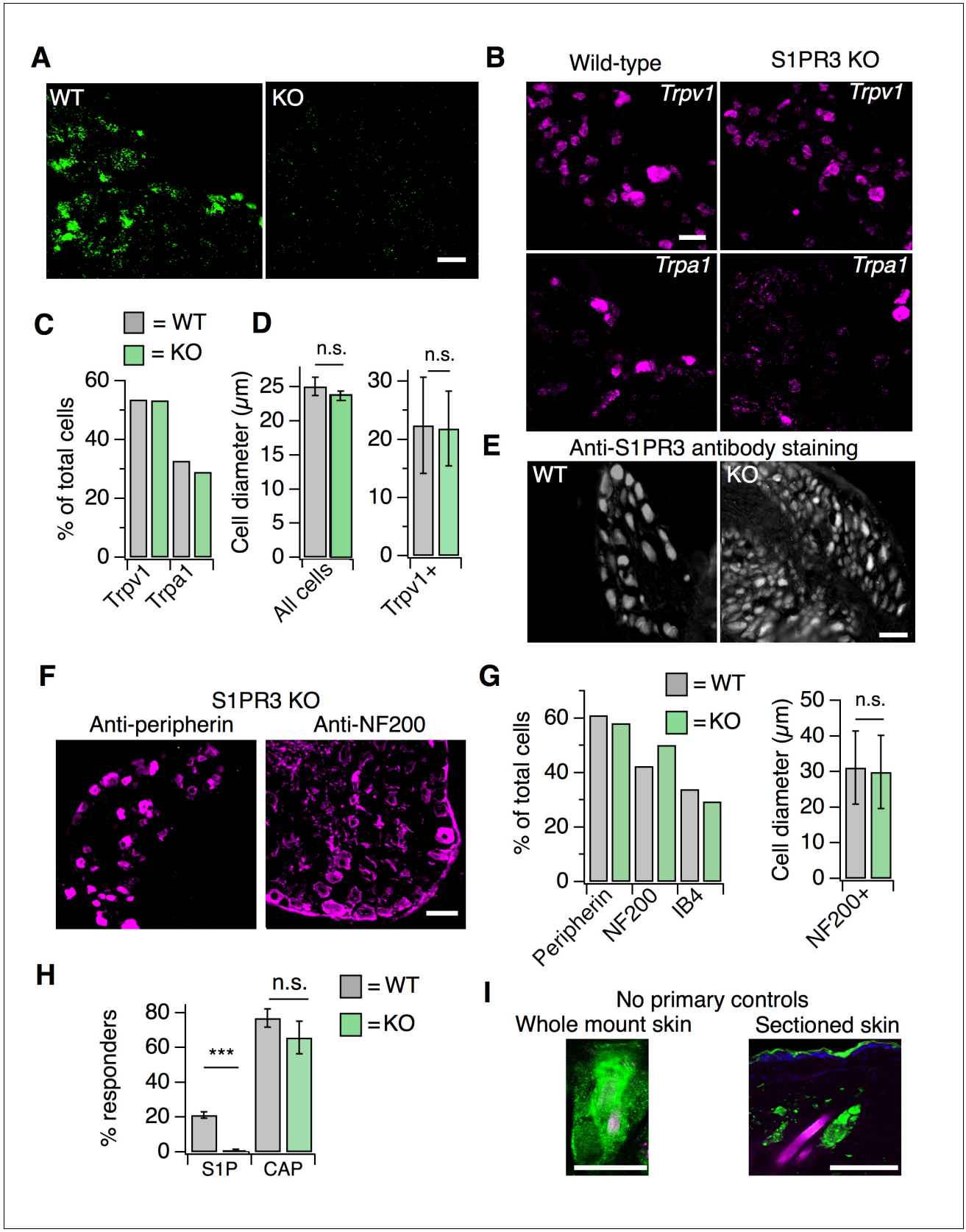

Figure 3—figure supplement 1. S1PR3 KO animals display normal representation of somatosensory neuronal subtypes. Related to ***Figure 3***. (**A**) ISH of sectioned adult DRG from WT and S1PR3 KO animals showing specificity of *S1pr3* probes (20x air objective, scale = 50 μm). (**B**) (Image) Representative

Figure 3—figure supplement 1 continued on next page

Figure 3—figure supplement 1 continued

ISH *Trpv1* (top) and *Trpa1* (bottom) from sectioned DRG of wild-type (left) and S1PR3 KO animals (right; 20x air objective; scale = 50 μm). (**C**) % of total cells expressing *Trpv1* and *Trpa1* in sectioned DRG of wild-type and S1PR3 KO animals. (**D**) (Left) Average diameter ± SEM of all cells in sectioned DRG from WT and S1PR3 KO animals (p=0.36, two-tailed t-test; n = 437 and 679 cells from two animals each, respectively). (Right) Average diameter ±SD of *Trpv1+* cells in WT and S1PR3 KO DRG (*p*=0.63, two-tailed t-test; n = 127 and 85 cells, respectively). (**E**) Representative staining with anti-S1PR3 antibody (1:2000) in sectioned adult DRG from WT and S1PR3 KO animals (10x air objective, scale = 100 μm). (**F**) Representative IHC images of sectioned DRG from S1PR3 KO animals stained with anti-DsRed (green) and anti-Peripherin (left, magenta) or anti-NF200 (right, magenta). Images were acquired using a 10x air objective (scale = 100 μm). (**G**) (Left) Quantification of total percentage of cells stained with indicated markers in sectioned DRG from $S1pr3^{mCherry/+}$ and S1PR3 KO animals (n > 250 cells per condition). (Right) Average diameter of anti-NF200 +cells in $S1pr3^{mCherry/+}$ and S1PR3 KO DRG (p=0.15, two-tailed t-test; n = 256 and 194 cells, respectively). (**H**) Percent responders to S1P and capsaicin in ratiometric calcium imaging of wild-type and S1PR3 KO cultured DRG and TG neurons; p<0.0001 (one-way ANOVA; N = 2 DRG and 2 TG preparations of 8 wells each). Sidak's multiple comparisons *p*-values are represented on graph for comparisons made between genotypes. Error bars represent mean ± SEM. (**I**) (Left) No primary control showing robust staining of hair follicles in whole mount skin in contrast to specific neuronal staining shown in ***Figure 3D***. (Right) No primary control showing staining around hair follicles and in epidermis in sectioned skin. Scale = 50 μm (20x water objective).

DOI: https://doi.org/10.7554/eLife.33285.008

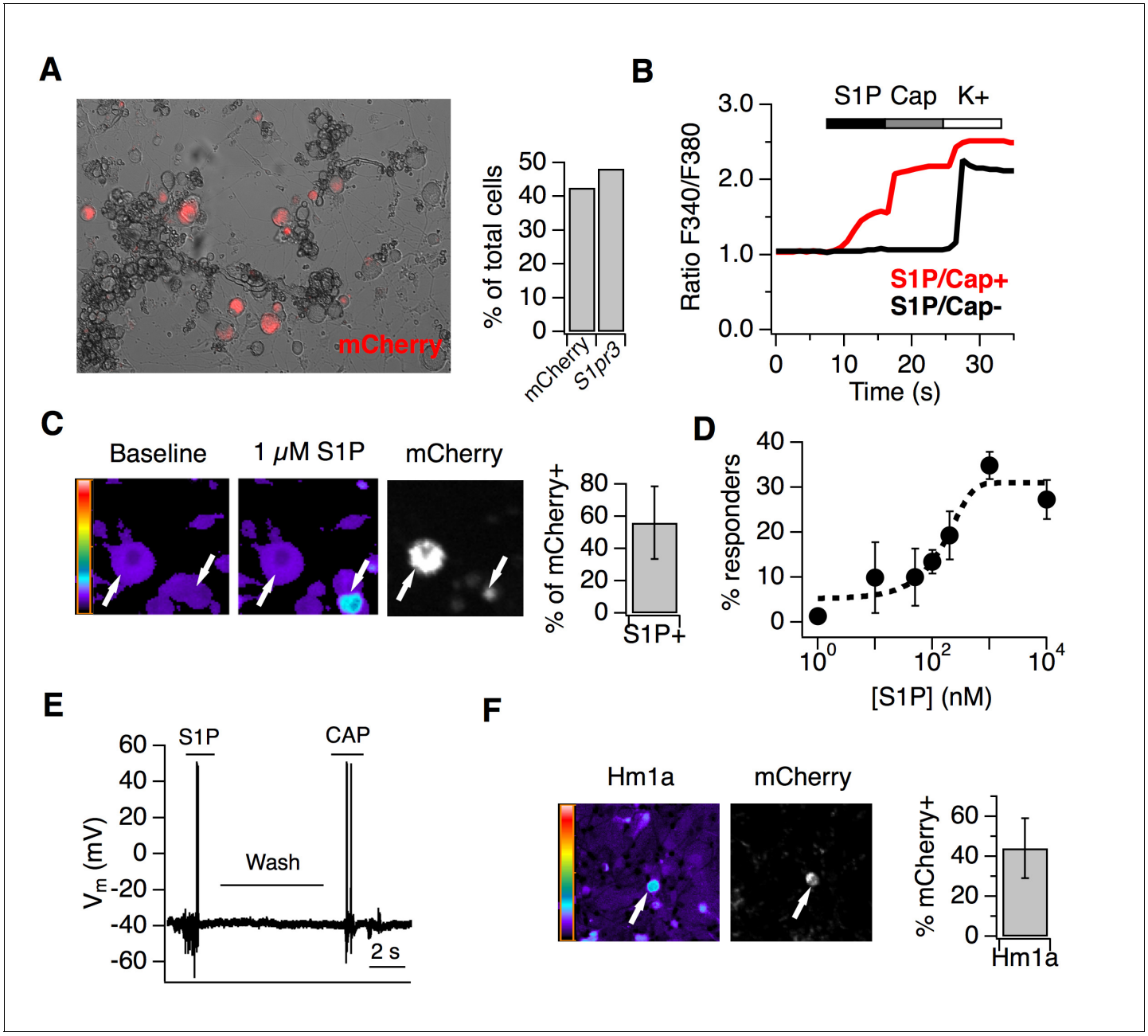

Figure 4. S1P activates thermal nociceptors but not mechanonociceptors. (**A**) (Left) Representative image of mCherry signal in live, cultured adult DRG neurons from one *S1pr3*$^{mCherry/+}$ animal. (Right) Quantification of % of total cells expressing *S1pr3* from DRG ISH and mCherry from dissociated DRG cultures (N = 2 animals each experiment). (**B**) Representative traces depicting F340/F380 signal from Fura2-AM calcium imaging showing two neurons, one which responded to 1 µM S1P, 1 µM Capsaicin, and high K + Ringer's (red) and one which only responded to high K+ (black). (**C**) (Left) Fura-2 AM calcium imaging before (left) and after (center) addition of 1 µM S1P in *S1pr3* $^{mCherry/+}$ cultured mouse DRG neurons. Bar indicates fluorescence ratio. Right-hand image indicates mCherry fluorescence. (Right) % of mCherry neurons that are responsive to 1 µM S1P in ratiometric calcium imaging (n > 1000 cells from 16 imaging wells from three animals). (**D**) Dose-response curve of mean neuronal calcium responders to varying concentrations of S1P. Concentrations used: 1, 10, 50, 100, 200, 1000, and 10,000 nanomolar (N = 2 animals). Error bars represent mean ± SD. Black dotted line indicates sigmoidal fit for all S1P responders from which EC_{50} was derived. All S1P responders were also capsaicin-responsive. (**E**) Current-clamp trace of a single wild-type neuron firing action potentials in response to bath addition of 1 µM S1P and 1 µM capsaicin, with Ringer's wash in-between. Four of tenneurons responded to S1P and one of one S1P-responsive also responded to capsaicin. Bar = 2 s. (**F**) (Left) Fura-2 AM calcium imaging after addition of 500 nM Hm1a in *S1pr3*$^{mCherry/+}$ P0 TG neurons, which were used instead of adult DRG neurons because they respond to Hm1a without prior PGE_2 sensitization. Right-hand image indicates mCherry fluorescence. (Right) % of Hm1a-responsive P0 TG neurons that are mCherry+ (N = 1 animal, 1230 total neurons).

DOI: https://doi.org/10.7554/eLife.33285.009

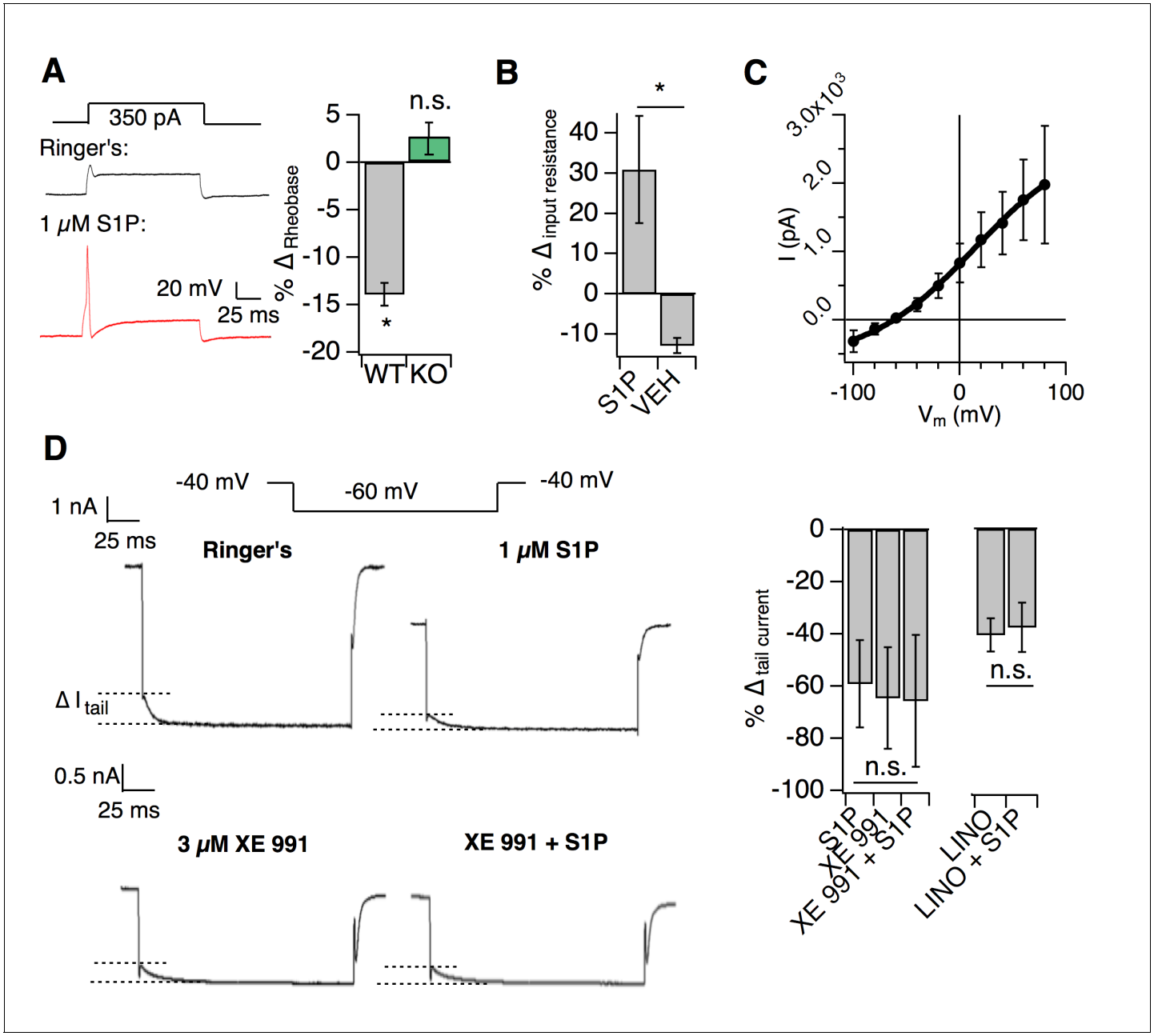

Figure 5. S1PR3 modulates KCNQ2/3 channels to regulate AM excitability. All experiments were performed in *S1pr3*$^{mCherry/+}$ or $^{-/-}$ DRG neurons. (**A**) (Left) Example traces of a single mCherry +neuron in whole cell current clamp before and after S1P application. (Right) % change in rheobase after S1P application for *S1pr3*$^{mCherry/+}$ (left, n = 7) and KO (right, n = 12) neurons ($p_{WT,KO}$ = 0.012, 0.287; two-tailed paired t-tests). (**B**) % Δ in input resistance after S1P or vehicle application (p=0.017; two-tailed paired t-test; n = 4 cells per group). (**C**) The S1P-sensitive current is carried by potassium. The current-voltage relationship was determined by subtraction of the post-S1P current from the pre-S1P current and reverses at −60.125 mV; n = 6 cells. Data were fitted with a Boltzmann equation. Pre- and post-S1P currents were measured at the indicated voltage (−100 mV to +80 mV, 20 mV increments) following a +100 mV step (100 ms). Current was quantified using the peak absolute value of the slowly-deactivating current 0–10 ms after stepping to indicated voltage. Unless indicated otherwise, all error bars represent mean ± SEM. (**D**) (Graphic, top) Averaged current traces of a single mCherry+ neuron in whole cell voltage clamp recording comparing tail currents ($\Delta_{I\ tail}$) pre- and post-S1P using indicated voltage step protocol. (graphic, bottom) Averaged current traces of a single mCherry+ neuron in whole cell voltage clamp recording with XE991 treatment. Holding phase (−40 mV, 150 ms) was truncated in traces. (Left graph) % Δ in outward tail current (average ±SD after indicated treatments (1 μM S1P, 3 μM XE 991, or both) for *S1pr3*$^{mCherry/+}$ medium-diameter neurons; (p=0.58; one-way ANOVA; n = 6, 8, 14 cells) using protocol depicted at right. (Right graph) % Δ in inward tail current after indicated treatments (LINO = 100 μM linopirdine) for *S1pr3*$^{mCherry/+}$ medium-diameter neurons; (p=0.47; two-tailed paired t-test; n = 12 cells).

DOI: https://doi.org/10.7554/eLife.33285.010

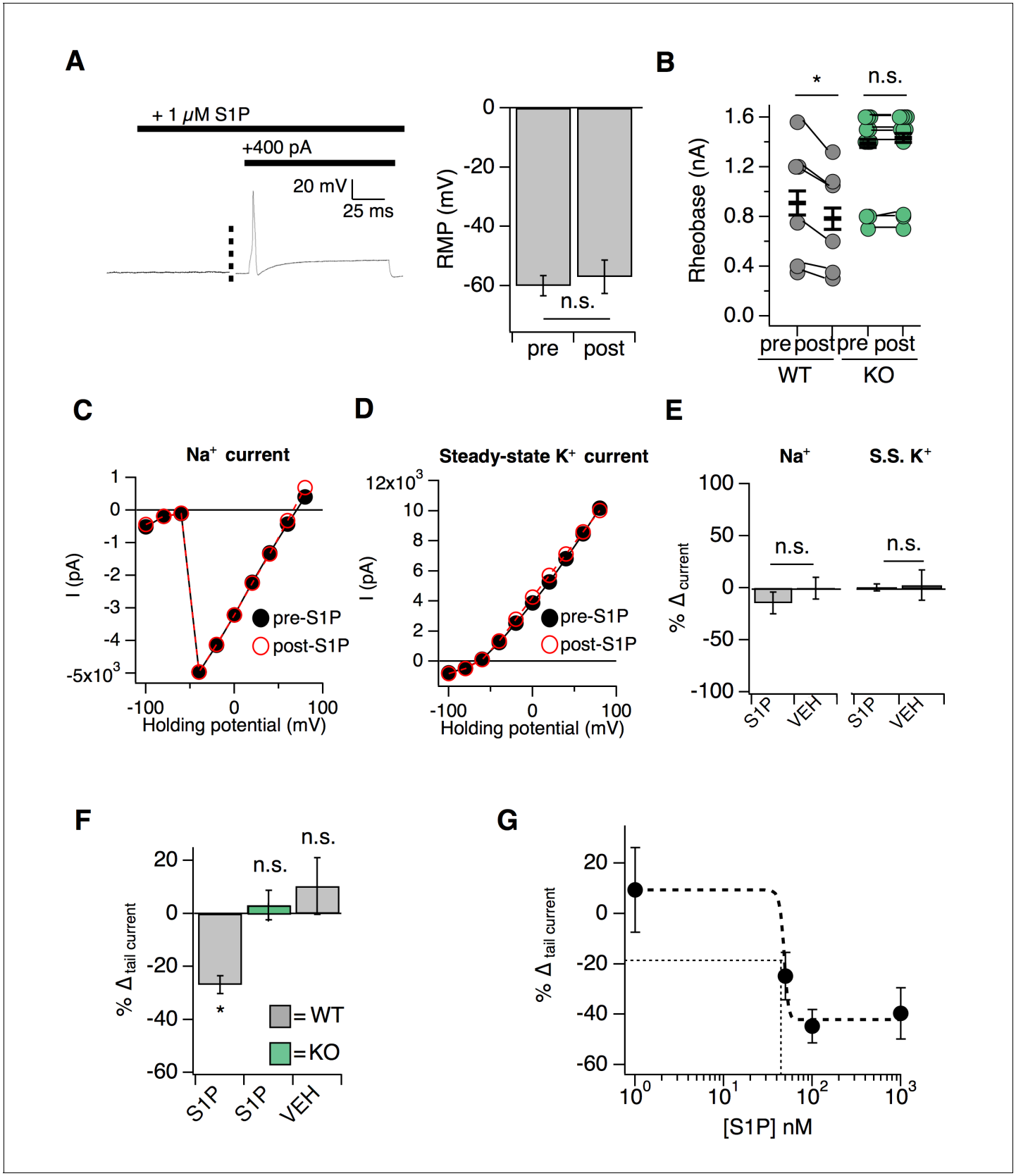

Figure 5—figure supplement 1. S1P selectively modulates potassium tail currents to increase DRG neuron excitability. Related to ***Figure 5***. (**A**) (Left) Example trace of a single mCherry+ neuron in S1P before and after current injection. (Right) Resting membrane potential (RMP) in millivolts before and

Figure 5—figure supplement 1 continued on next page

Figure 5—figure supplement 1 continued

after addition of S1P (p=0.23; two-tailed paired t-test; n = 6 cells). (**B**) Rheobase pre- and post-S1P application in DRG neurons; p_{WT} = 0.011; p_{KO} = 0.28 (two-tailed paired t-test). Same data are represented in ***Figure 5A***. (**C**) Sodium I-V relationship for a representative *S1pr3*$^{mCherry/+}$ medium-diameter neuron pre- and 5 min post- 1 µM S1P using voltage step from −100 to +80 mV (150 ms steps, −80 mV holding). (**D**) Steady-state I-V relationship for same neuron. (**E**) (Left) % Δ in peak sodium current (Na^+) after S1P or 1% DMSO vehicle application for medium-diameter mCherry+ neurons; p=0.39 (two-tailed paired t-test; n = 7 cells per group). (Right) % Δ in peak steady-state current (S.S. K^+) after S1P or 1% DMSO vehicle application for medium-diameter mCherry+ neurons; p=0.948 (two-tailed paired t-test; n = 7 cells per group). (**F**) % Δ in inward tail current ($\Delta_{I\ tail}$) after S1P or 1% DMSO vehicle application for *S1pr3*$^{mCherry/+}$ and KO medium-diameter neurons using a pre-pulse stimulation of +80 mV followed by a step to −80 mV, where ($\Delta_{I\ tail}$) was calculated by subtracting the steady-state current from the absolute peak of the slowly-deactivating current at −80 mV (p=0.014; one-way ANOVA; n = 10, 13, 10 cells). Tukey Kramer post hoc *p*-values indicated on graph. (**G**) Dose-response relationship between % Δ in tail current and S1P concentration for 1 nM, 50 nM, 100 nM, and 1 µM S1P (n = 7 cells). EC_{50} (48.8 nM), marked by thin dotted lines, was estimated from sigmoidal fit (thick dotted line).

DOI: https://doi.org/10.7554/eLife.33285.011

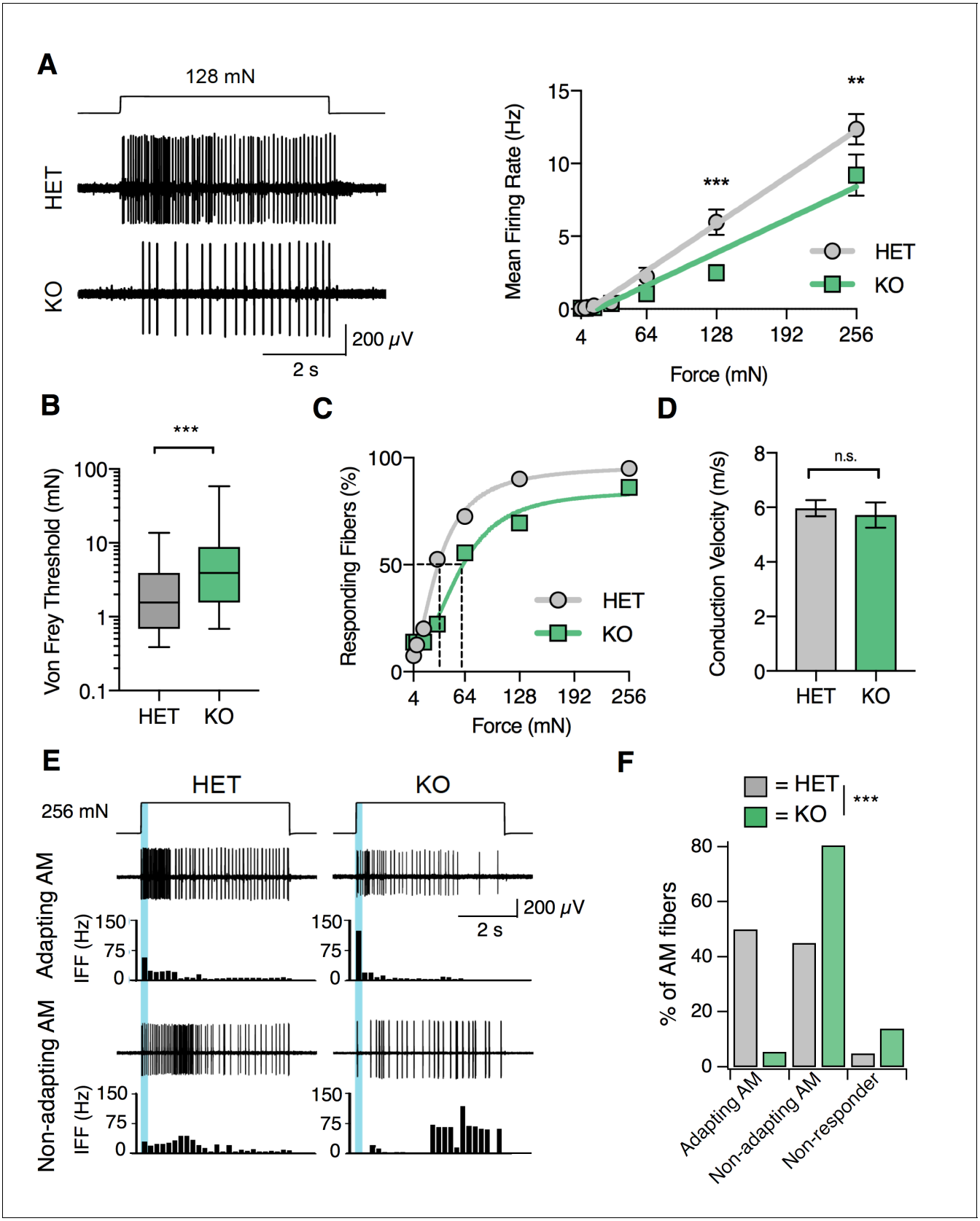

Figure 6. S1PR3 is required for nociceptive responses of high-threshold AM nociceptors. (**A**) (Left) Representative traces of AM fiber activity over time in ex vivo skin-saphenous nerve recording in response to stimulation (128 mN, top) from HET (middle) and KO (bottom) mice. (Right) Mean firing rate of

Figure 6 continued on next page

Figure 6 continued

AM fibers in response to force controlled stimulation (4, 8, 16, 32, 64, 128, 256 mN). **p=0.001, ***p=0.0002 (two-way ANOVA, Sidak's post-hoc); lines, linear regression (HET: slope = 50 Hz/N, R^2 = 0.99; KO: slope = 35 Hz/N, R^2 = 0.95). (**B**) von Frey threshold of AM fibers in S1PR3 HET and KO specimens. ***p<0.0001 (Mann-Whitney test); lines, median; boxes, 25–75 percentile; whiskers, min-max. (**C**) Cumulative response plot of AM fibers to force controlled stimulation (solid lines); four-parameter logistic fit from which half-maximal force was estimated for each genotype (dotted lines). (**D**) Conduction velocity (CV) of AM fibers in S1PR3 HET and KO mice. p=0.65 (two-tailed t-test); n = 40, 36 fibers; errors, mean ± SEM. (**E**) Representative traces and binned instantaneous firing frequencies (IFF; 200 ms bins) of Non-Adapting and Adapting AMs in response to force controlled stimulation (256 mN, top) for S1PR3 HET and KO mice; blue regions, dynamic phase of stimulation (200 ms). (**F**). Proportion of fibers classified by pattern of mechanically evoked responses to 256-mN stimuli: Non-Responder (HET, 2/40 fibers; KO 5/36), Non-Adapting AM (HET, 18/40; KO, 29/36), Adapting AM (HET, 20/40; KO, 2/36). Non-Responders fired action potentials to large magnitude von Frey monofilaments (<0.5 mm tip diameter), but not controlled mechanical stimulation (256 mN, 2 mm tip diameter). ***p<0.00001 (Chi-square test).

DOI: https://doi.org/10.7554/eLife.33285.013

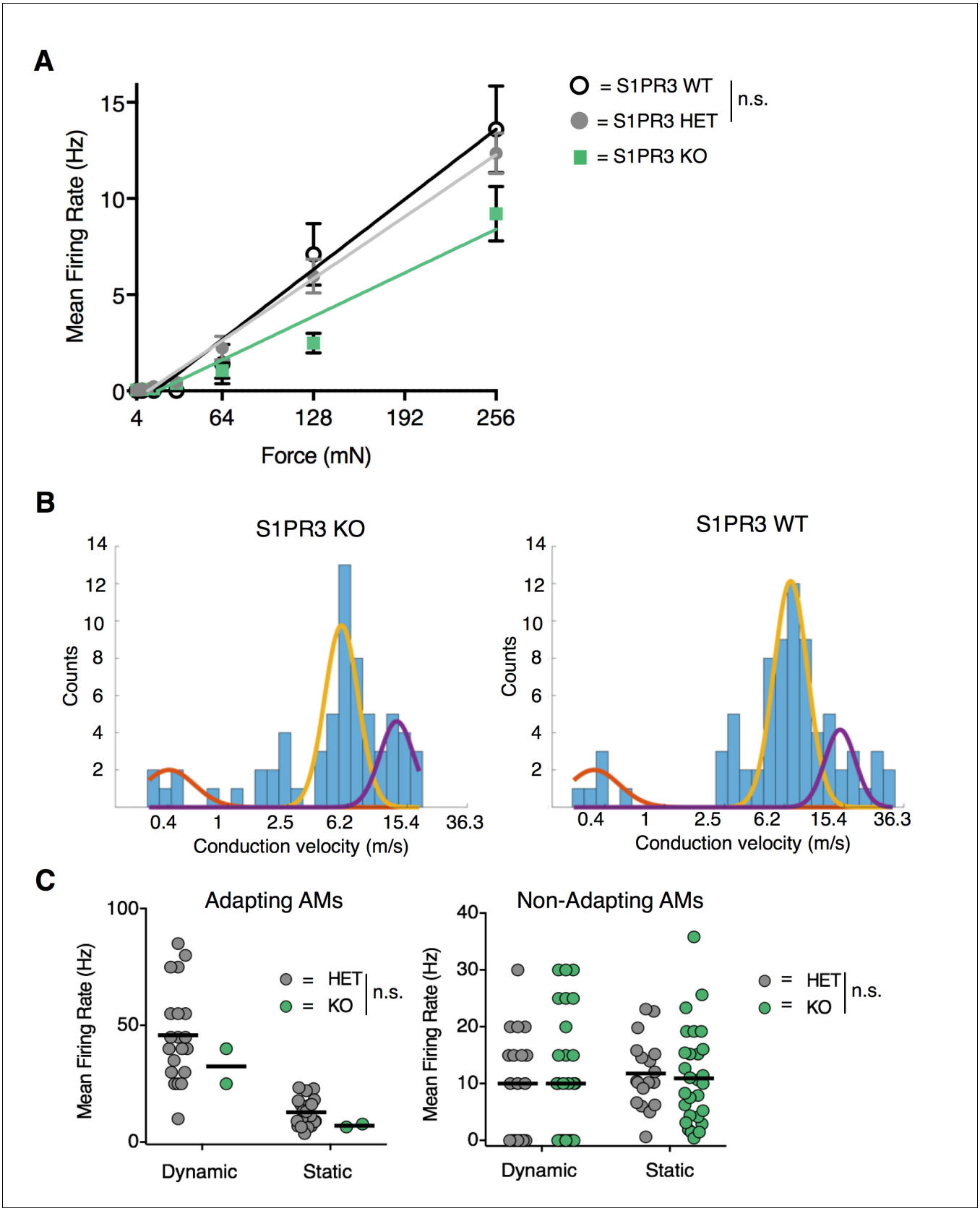

Figure 6—figure supplement 1. S1PR3 HET AM nociceptors display normal nociceptive responses. Related to ***Figure 6***. (**A**) Mean firing rate of AM fibers in response to force controlled stimulation (4, 8, 16, 32, 64, 128, 256 mN) from ***Figure 6A***, with additional data from one wild-type animal

Figure 6—figure supplement 1 continued on next page

Figure 6—figure supplement 1 continued

(n_{WT} = 4 fibers) (WT: slope, 57 Hz/N, R (***Vriens et al., 2011***), 0.98; p=0.90, two-way ANOVA comparing HET and WT). (**B**) (Left) Conduction velocities from teased fibers from 6 S1PR3 KO animals (purple, Aβ, centroid = 13.1 m/s; yellow, Aδ, centroid = 5.7 m/s; orange, C, centroid = 0.4 m/s; R^2 = 0.69, N = 65 fibers). (Right) Conduction velocities from teased fibers from 1 S1PR3 HET and 6 C57BL/6 WT animals (purple, Aβ, centroid = 14.5 m/s; yellow, Aδ, centroid = 6.8 m/s; orange, C, centroid = 0.3 m/s; R^2 = 0.82, N = 76 fibers). Three-term Gaussian model. X-axis plotted on a log 1.2 scale. (**C**) Mean firing rates during dynamic (ramp) and static (hold) stimulation for S1PR3 HET and S1PR3 KO recordings (left, Adapting AMs; right, Non-Adapting AMs; see ***Figure 6E–F*** for experimental details). No significant differences were found between genotypes (p=0.227, 0.490 (two-way ANOVA); bars, means). As shown in ***Figure 6F***, the proportion of Adapting AMs was significantly lower in S1PR3 KO recordings compared with littermate controls.

DOI: https://doi.org/10.7554/eLife.33285.014

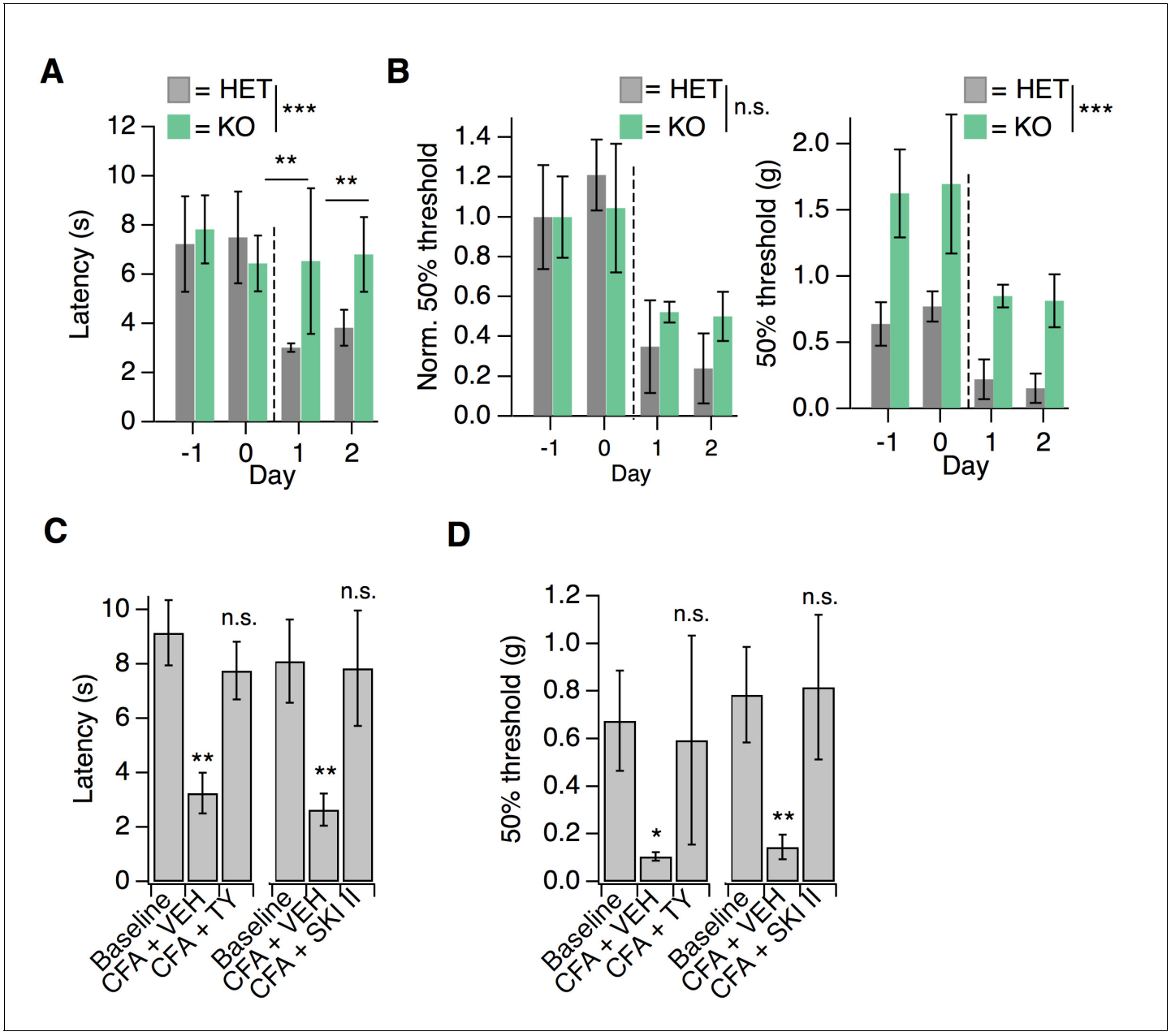

Figure 7. S1PR3 is dispensable for development of chronic mechanical hypersensitivity. (**A**) Thermal latency before and after CFA treatment (indicated by dotted line); $p_{genotype}$ = 0.0053 (two-way ANOVA; N = 5 mice per genotype). Sidak's multiple comparison between genotypes for specific time points indicated on graph. Error bars represent mean ± SD. (**B**) (Left) Normalized 50% withdrawal threshold before and after CFA treatment (indicated by dotted line); *p*(genotype)<0.001 (two-way ANOVA). (Right) 50% withdrawal thresholds for same experiment (*p*(genotype)=0.1634; two-way ANOVA). (**C**) (Left) Thermal latency assessed before ('Baseline') and 24 hr post CFA injection with either vehicle (CFA + VEH) or TY 52156 (CFA + TY) acutely administered; p<0.0001 (one-way ANOVA N = 5 mice per treatment). (Right) Thermal latency assessed before and after CFA injection with either vehicle (CFA + VEH) or SKI II (CFA + SKI II) acutely administered on Day 1; p<0.0001 (one-way ANOVA; N = 5–7 mice per treatment). Dunnett's test comparisons to baseline are indicated on graph. Error bars represent mean ± SD. (**D**) (Left) 50% withdrawal threshold assessed before and 24 hr post CFA injection with either vehicle (CFA + VEH) or TY 52156 (CFA + TY) acutely administered on Day 1; p<0.0001 (one-way ANOVA; N = 5 mice per treatment). Dunnett's test comparisons to baseline are indicated on graph. (Right) 50% withdrawal threshold assessed before and 24 hr post CFA injection with either vehicle (CFA + VEH) or SKI II (CFA + SKI II) acutely administered; *p*-values indicated on graph (two-tailed unpaired t-test; N = 5 mice per group.

DOI: https://doi.org/10.7554/eLife.33285.016

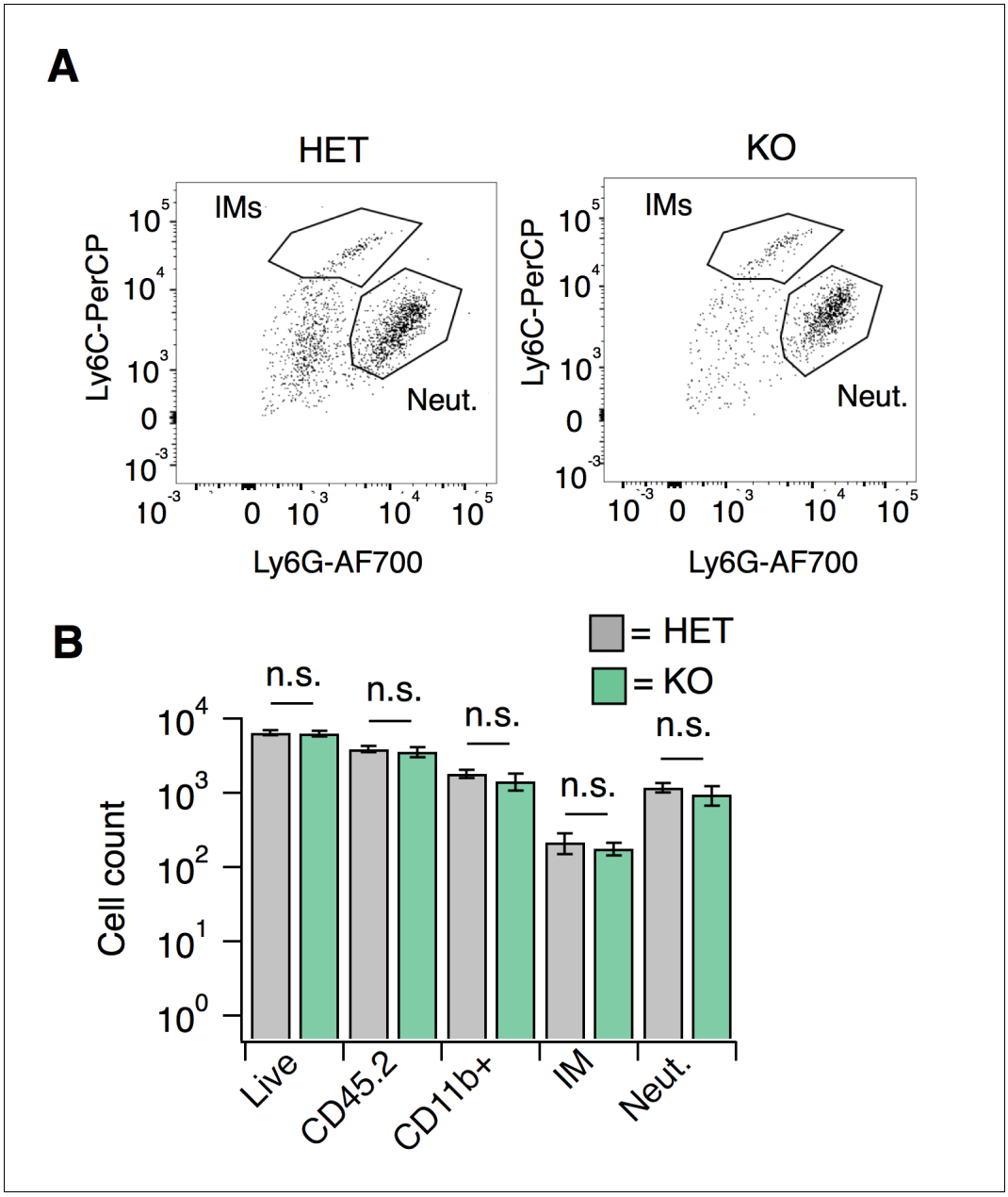

Figure 7—figure supplement 1. S1PR3 KO animals display normal CFA-evoked immune cell recruitment. Related to ***Figure 7***. (**A**) Recruitment of neutrophils (Neut.) or inflammatory monocytes (IMs) to hindpaw skin 24 hr post-CFA administration in S1PR3 HET and KO mice, as a dot plot of CD11b + cells plotting Ly6G fluorescence intensity vs. Ly6C intensity (AFU). Boxes are for illustrative purposes. (**B**) Recruitment of immune cells, including neutrophils (Neut.) and inflammatory monocytes (IMs) to hindpaw skin 24 hr post-CFA administration in HET and KO mice, displayed as total number of cells; N = 8 mice per genotype. Sidak's multiple comparisons were made between HET and KO for each cell type.

DOI: https://doi.org/10.7554/eLife.33285.017

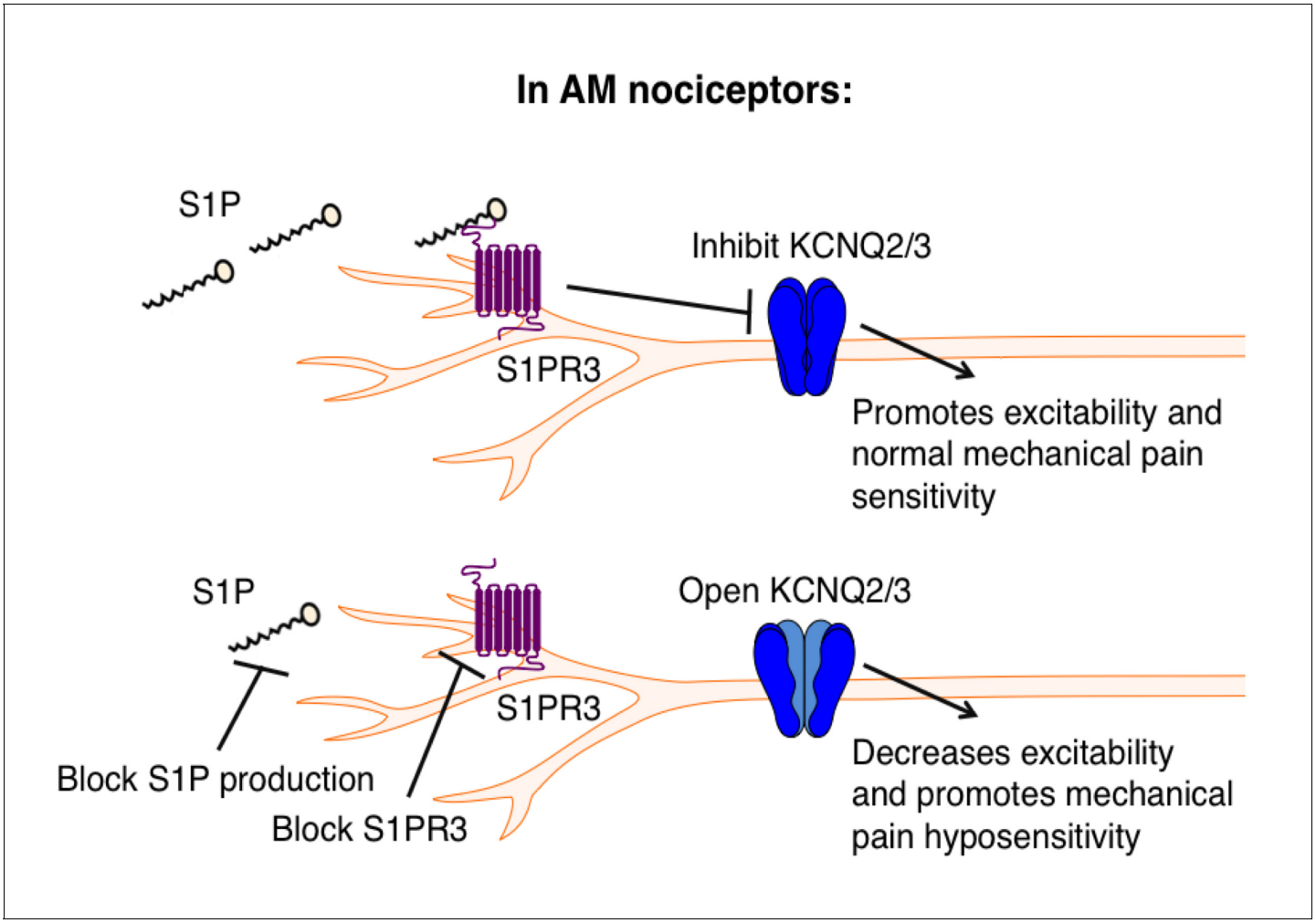

Figure 8. Proposed model illustrating a key role for S1PR3 in regulating mechanical pain in AM nociceptors. (Top) S1P promotes activation of S1PR3, which leads to inhibition of KCNQ2/3 currents and promotes normal mechanical pain sensitivity. (Bottom) Diminished S1P or S1PR3 antagonism alleviates inhibition of KCNQ2/3, leading to mechanical pain hyposensitivity.

DOI: https://doi.org/10.7554/eLife.33285.019